Supporting Information

Dupont et al. 10.1073/pnas.0905444107

SI Materials and Methods

Scaffold Preparation. Poly(ε-caprolactone) (PCL) cylindrical scaffolds, 9 mm in height, 5 mm in diameter, and of 85% porosity were punched from PCL sheets (Osteopore International) using dermal biopsy punches. The scaffolds feature a honeycomb array of layers of interconnected struts oriented in a repeated lay-down pattern of 0°/60°/120°. Scaffolds were sterilized by ethanol evaporation, soaked in a 50 μg/mL solution of the collagen-mimetic peptide GFOGER overnight at 4 °C, and coated with 1.5 mg/mL lyophilized type I collagen (Vitrogen 100; Cohesion Technologies) to increase cell adhesion and help mediate the osteogenic response of MSCs (1) and AFS cells.

Cell Culture. Human MSCs (passages 3–4) were a gift from Tulane University and were originally isolated from bone marrow aspirates as described in ref. 2. Human AFS cells (passages 18–19) were a gift from the Wake Forest University Institute for Regenerative Medicine and were originally isolated from human amniotic fluid as described in ref. 3. Rat MSCs (passage 3) were isolated from long bone marrow aspirates as described in ref. 4. Non–stem cell control human embryonic kidney 293 (HEK) cells (passage 34) were purchased from American Type Culture Collection.

For segmental defect studies, hMSCs and hAFS cells were seeded on tissue culture plates and grown to near-confluence in culture media [α-MEM, 16.7% FBS (Atlanta Biologicals), penicillin/streptomycin/L-glutamine (PSL) (Invitrogen)]. Equal numbers of cells from two human donors were combined for each stem cell source. For QD segmental defect studies, 3 million hMSCs or hAFS cells were seeded on 15-cm-diameter culture dishes while 3 million HEK cells were seeded on T-150 flasks and incubated overnight in 20 mL of medium (stem cells: α-MEM, 16.7% FBS, PSL; HEK cells: DMEM, 10% FBS, PSL). Cells were then incubated in a 5 nM solution of QTracker 800 quantum dots (Invitrogen) in 5 mL of culture medium for 18 h and then trypsinized and counted. Either 3 million (hMSCs/hAFS cells) or 6 million (hMSCs/HEK) QD-labeled cells in 100 μL of culture medium were seeded onto PCL scaffolds as described above, and scaffolds were cultured at 37 °C/5% CO_2 until implantation 24 h later. Some QD-labeled hMSC scaffolds were exposed to devitalizing freeze–thaw cycles after a 24-h culture consisting of three repetitions of freezing at −80 °C for 30 min followed by thawing at 37 °C for 30 min in a water bath. For the defect study without QDs, cells were seeded on scaffolds and cultured until implantation 2 days later.

For 2D in vitro QD studies, 20,000 rMSCs were seeded in each well of eight-well Lab-Tek chambered cover glass plates in 300 μL of culture medium, allowed to adhere overnight, and loaded with 5, 10, or 20 nM solutions of QTracker 800 QDs or QDot ITK 800 QDs (Invitrogen) for either 1 h or 18 h. Both types of QDs have peak fluorescent emission at the 800-nm wavelength, which enables avoidance of in vivo autofluorescent background signals because the major chromophores in mammals, hemoglobin and water, have local minima in absorption in this wavelength range (5, 6). The QTracker QDs feature amino-PEGylation surface coatings giving them a positive charge, whereas the QDot ITK QDs are coated with carboxyl surface groups giving them a negative charge, and both types of QDs are passively endocytosed into the cytoplasmic spaces of cells. After QD incubation, cells were washed with PBS, fixed with formalin, and washed with PBS again before imaging. Additionally, some of the wells incubated in 10 nM QDs were stained for 5 min with 5 ng/mL DAPI nuclear stain. Next, rMSCs, hMSCs, and hAFS cells were loaded with QDs as described above but at concentrations of 0, 10, 15, and 20 nM, and all were incubated for 18 h. All wells were fixed and stained with DAPI. Additionally, stem cells in other eight-well plates were loaded with QDs in the same manner but were not fixed or stained with DAPI; instead, they were washed with PBS and then stained with Live/Dead stain (consisting of calcein/ethidium; Invitrogen) for 45 min to assess cell viability. To assess QD effects on osteogenic differentiation, 1,000 hMSCs were seeded in the wells of tissue culture six-well plates and grown to confluence. 0.5 mL of 5 nM QTracker QDs were then added to half of the wells for 18 h while the other wells received 0.5 mL of culture media. Next, wells were aspirated and 5 mL of culture media supplemented with osteogenic factors (1 nM dexamethasone, 6 mM β-glycerol phosphate, 50 μg/mL ascorbic acid 2-phosphate, 50 ng/mL L-thyroxine) was added. Plates were cultured for 3 weeks with media changes twice weekly, and then a Von Kossa assay was performed to assess mineral formation.

For 2D in vitro human cell nuclear labeling, 100,000 hMSCs were seeded on single-well Lab-Tek chambered cover glass slides and allowed to adhere overnight. Cells were fixed in formalin, permeabilized with acetone, and blocked in 5% donkey serum followed by application of a mouse anti-human nuclear antigen monoclonal antibody (HuNu) (Millipore, MAB1281). Next, a fluorescent Alexa Fluor 488 donkey anti-mouse (Invitrogen) secondary antibody was applied, followed by DAPI counter staining.

DNA Analysis. Three days after seeding cells for the segmental defect studies as mentioned above, scaffolds with cells were removed from culture to quantify DNA ($n = 5$ / stem cell source). Scaffolds were washed with PBS and dried overnight in a speed vacuum (DNA SpeedVac 120, Thermo Scientific). Next scaffolds were digested with Proteinase K, followed by DNA quantification using a PicoGreen assay (Quant-iT PicoGreen dsDNA Kit; Invitrogen) and fluorescence plate reader (PerkinElmer, HTS 7000).

Surgical Technique. All surgical techniques were approved by the Georgia Institute of Technology Institutional Animal Care and Use Committee (Protocol A08032). Female 13-week-old athymic rats (RNU Nude, Charles River Laboratories, Wilmington, MA) were anesthetized using isoflurane. Bilateral 8-mm critically sized femoral defects were then created and stabilized by novel custom modular fixation plates developed in our laboratory and described previously (7, 8). In the QD-free study, PCL scaffolds, with or without cells, were press fitted into the defects before closing the wound site. Rats received a balanced bilateral combination of either acellular scaffold ($n = 8$), hMSC-seeded scaffold ($n = 9$), or hAFS cell-seeded scaffold ($n = 9$). In both of the in vivo QD studies, all rats were implanted with scaffolds containing QD-labeled cells in one hindlimb defect and acellular scaffolds only in the contralateral defect. In the preliminary QD study, two rats were treated with hMSCs and two rats with hAFS cells. In the QD study comparing live and devitalized cells, 10 rats were treated with scaffolds containing live hMSCs ($n = 5$ 3E6 cells/$n = 5$ 6E6 cells), 10 rats were treated with scaffolds containing devitalized hMSCs ($n = 5$ 3E6 cells/$n = 5$ 6E6 cells), and 2 rats were treated with 6E6 HEK cells. Rats were given s.c. injections of 0.04 mg/kg buprenorphine every 8 h for the first 48 h postsurgery and 0.013 mg/kg buprenorphine every 8 h for the following 24 h for pain relief. Animals resumed normal ambulation and behavior within three days, except for one rat in the preliminary QD study

that failed to recover because of misplacement of the internal fixator plate, leading to its euthanization after 4 days.

X-Ray and Microcomputed Tomography (Micro-CT) Imaging. Qualitative bone growth into defect sites was assessed by 2D in vivo digital x-rays (Faxitron MX-20 Digital; Faxitron X-Ray) taken at 4, 8, and 12 weeks postsurgery after rats were anesthetized with isoflurane. For the QD-free study and the QD study comparing live and devitalized cells, quantitative bone formation was assessed by 3D microcomputed tomography scans (Viva-CT 40; Scanco Medical) both in vivo at 8 and 12 weeks postsurgery and by postmortem ex vivo scans. Micro-CT is a fast and nondestructive technique that can be used to characterize and measure the 3D properties of scaffold/tissue composites during bone regeneration (9). After application of isoflurane anesthesia, the live rats were positioned in a custom scanning chamber to isolate the defects in the center of the scanning region. Rats were killed after 12 weeks, and femurs were carefully excised along with surrounding soft tissue, wrapped in PBS-soaked gauze, and frozen at −20 °C until postmortem scanning. At the time of postmortem scans, femurs were thawed in PBS, placed in 15-mL microcentrifuge tubes filled with PBS, and scanned by Micro-CT. A 38.5-μm voxel resolution was used, and after scanning a constant volume of interest (VOI) was centered over the defect site for quantitative analysis of samples. For in vivo scans, a VOI ≈4 mm long centered in the middle of the defect region was chosen to ensure measurement of new bone formation and avoid measuring native cortical bone ends. A Gaussian filter was used to suppress noise, and a density threshold corresponding to 272 mg of hydroxyapatite/cm^3 was used to discriminate bone from soft tissues and polymer.

Torsional Mechanical Testing. For both the QD-free study ($n = 8$ acellular scaffold group, $n = 9$ per stem cell group) and the QD live versus devitalized cells study ($n = 9$ each for the live, live contralateral, devitalized, and devitalized contralateral groups), immediately following post mortem Micro-CT imaging femurs were carefully cleaned of remaining soft tissue. Bone ends were potted in custom mounting blocks that contained reservoirs of heated Wood's Metal (Alfa Aesar), an alloy that melts at low temperatures and quickly solidifies after potting of bone ends. The mounting blocks were then loaded onto an ELF 3200 ElectroForce torsion testing system (Bose Corporation). Next, the polysulfone bridging plate, which had shielded defects from loads and damage, was removed by unscrewing four screws attaching it to two stainless steel plates, each of which was screwed into to the native femoral bone on either side of the defect site. Finally, a rotation-controlled torsional load was applied to the femur at a rate of 3°/sec, and maximum torque and torsional stiffness were recorded through 90° rotation.

Preparation of Histological Cryosections. All rats from the preliminary QD study were killed 12 weeks after surgery and had their femurs, kidneys, and organs of the reticuloendothelial system (spleen, liver, lymph nodes) harvested. Femurs were decalcified in Cal-Ex solution, and then all tissues were fixed in 10% neutral buffered formalin, embedded in OCT cryosectioning medium, and snap frozen in a chilling bath. Fifty-micrometer tissue sections were taken by using a Microm Cryo-Star HM 560MV cryostat (Thermo Fisher) and attached to Superfrost Plus slides. Glass coverslips were mounted using ProLong Gold antifade mounting medium with DAPI (Invitrogen) to visualize cell nuclei. In the live versus devitalized cell QD study, one rat each from the live hMSC group, devitalized hMSC group, and HEK group (each 6E6 cells) was killed 4 weeks after surgery. Animals were chosen that displayed average defect fluorescence intensity per group as assessed by IVIS scan quantification. Femurs were collected, embedded in OCT media, snap-frozen, and then sectioned in 20-μm slices. All sections were fixed in 4% formaldehyde in PBS. Sections prepared for human nuclei staining were blocked with 5% donkey serum followed by application of HuNu primary antibody (Millipore, MAB1281). Sections prepared for rat macrophage staining were blocked with 5% BSA followed by application of a mouse anti-rat CD68 primary antibody (AbD Serotec, MCA341R). Next, a fluorescent Alexa Fluor 488 donkey anti-mouse (Invitrogen) secondary antibody was applied to all sections followed by DAPI counter staining. Control sections for each immunolabel excluded primary antibody staining.

Fluorescence Microscopy. Fluorescent images of cells in Lab-Tek plates and of tissue cryosections were obtained by using a Zeiss Axio Observer inverted microscope (Zeiss) equipped with a specialized Qdot 800 filter set (Chroma 32021; Chroma Technology).

IVIS Fluorescent Imaging. Macroscopic fluorescent images of eight-well plates were obtained using an IVIS Lumina fluorescent imaging system (Caliper Life Sciences) capable of quantifying fluorescence emission levels. Image settings consisted of small binning, an f-stop of 2, 60 sec of excitation, and 745/800-nm excitation/emission wavelengths. For the preliminary in vivo study, fluorescent scans were performed on isoflurane-anesthetized rats immediately after surgery and then weekly for 12 weeks. For the live versus devitalized cell study, scans were performed immediately postoperative and then after 10, 20, 40, 60, and 80 days. Image settings consisted of medium binning, an f-stop of 1, 13 sec of excitation, and 710/800-m excitation/emission wavelengths. Fluorescent count values were measured by using a uniform circular region of interest applied at hindlimb defect sites.

Statistical Analysis. For the comparison of defect bone volume and mechanical properties, one-way analysis of variance was performed in Minitab (Minitab Inc.) using a general linear model with Tukey pairwise post hoc tests for statistical comparison of data. For the comparison of defect site QD fluorescence, repeated-measures two-way analysis of variance was performed with Bonferroni post tests in Prism 5 (GraphPad Software).

1. Reyes CD, Petrie TA, Burns KL, Schwartz Z, García AJ (2007) Biomolecular surface coating to enhance orthopaedic tissue healing and integration. *Biomaterials* 28:3228–3235.
2. Sekiya I, et al. (2002) Expansion of human adult stem cells from bone marrow stroma: conditions that maximize the yields of early progenitors and evaluate their quality. *Stem Cells* 20:530–541.
3. De Coppi P, et al. (2007) Isolation of amniotic stem cell lines with potential for therapy. *Nat Biotechnol* 25:100–106.
4. Hofstetter CP, et al. (2002) Marrow stromal cells form guiding strands in the injured spinal cord and promote recovery. *Proc Natl Acad Sci USA* 99:2199–2204.
5. Lim YT, et al. (2003) Selection of quantum dot wavelengths for biomedical assays and imaging. *Mol Imaging* 2:50–64.
6. Smith AM, Duan H, Mohs AM, Nie S (2008) Bioconjugated quantum dots for in vivo molecular and cellular imaging. *Adv Drug Deliv Rev* 60:1226–1240.
7. Oest ME, Dupont KM, Kong HJ, Mooney DJ, Guldberg RE (2007) Quantitative assessment of scaffold and growth factor-mediated repair of critically sized bone defects. *J Orthop Res* 25:941–950.
8. Rai B, et al. (2007) Combination of platelet-rich plasma with polycaprolactone-tricalcium phosphate scaffolds for segmental bone defect repair. *J Biomed Mater Res A* 81: 888–899.
9. Jones AC, et al. (2004) Analysis of 3D bone ingrowth into polymer scaffolds via micro-computed tomography imaging. *Biomaterials* 25:4947–4954.

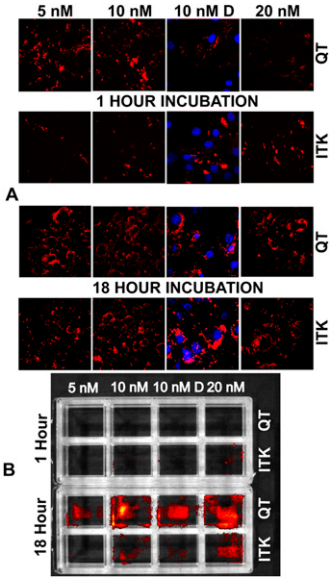

Fig. S1. Fluorescence emission from QD-labeled rat MSCs in 2D culture as seen in fluorescence microscopy images (*A*) and IVIS Lumina fluorescence scans (*B*). Note the presence of red QDs in cytoplasmic space surrounding blue nuclei counterstained with DAPI in *A* (magnification, 40×). QT, QTracker 800 QDs; ITK, QDot ITK 800 QDs.

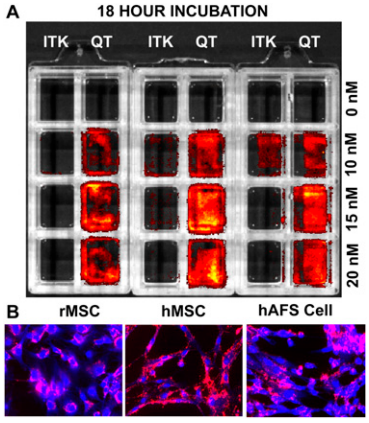

Fig. S2. Comparison of fluorescence emission from rMSCs, hMSCs, and hAFS cells as assessed by either IVIS imaging (*A*) or fluorescence microscopy (*B*). Microscopy images shown for 10 nM QD concentration. (Magnification: 20×.)

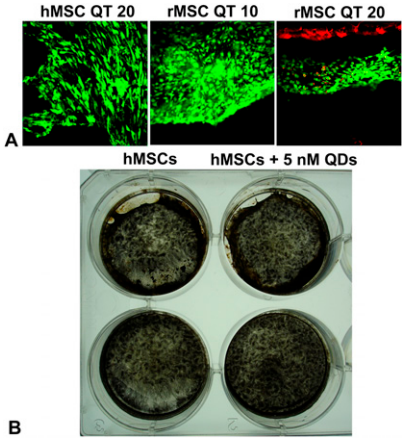

Fig. S3. QD effects on 2D in vitro stem cell behavior. (*A*) Viability: fluorescence microscopy images showing presence of live (green) and dead (red) cells after Live/Dead stain. QDs only had negative effects on stem cell viability in the well containing rMSCs loaded with 20 nM QDs. (Magnification: 10×.) (*B*) Osteogenic differentiation: the presence of QDs did not qualitatively reduce mineral formation from hMSCs.

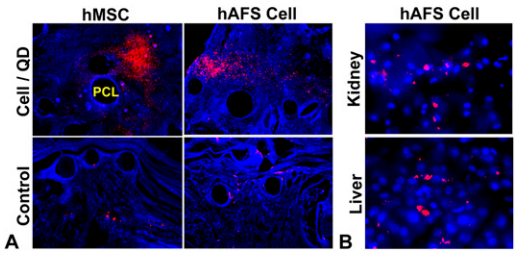

Fig. S4. Quantum dot fluorescence in histological cryosections—preliminary study. (*A*) Quantum dots (red) and DAPI-stained cells (blue) within pore spaces of PCL scaffolds delivered to bone defect sites. (Magnification: 4×.) (*B*) Quantum dots found within liver and kidney harvested after 12 weeks. (Magnification: 63×.)